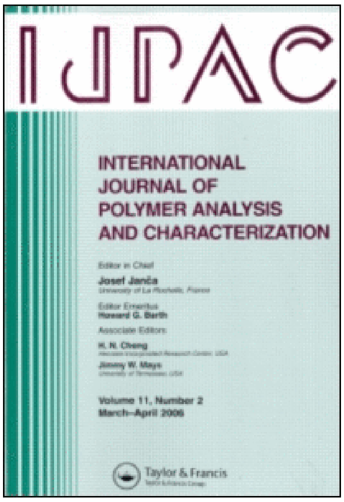

International Journal of Polymer Analysis and Characterization
Publication details, including instructions for authors and subscription information:
http://www.informaworld.com/smpp/title~content=t713646643

Dynamic Light Scattering from Multicomponent Polymer Solutions

T. P. Lodge[a]
[a] Department of Chemistry, University of Minnesota, Minneapolis, MN

To cite this Article Lodge, T. P.(1996) 'Dynamic Light Scattering from Multicomponent Polymer Solutions', International Journal of Polymer Analysis and Characterization, 2: 4, 323 — 334

To link to this Article: DOI: 10.1080/10236669608033353

URL: http://dx.doi.org/10.1080/10236669608033353

Int. J. Polymer Analysis & Characterization
1996, Vol. 2, pp. 323–334
Reprints available directly from the publisher
Photocopying permitted by license only

Dynamic Light Scattering from Multicomponent Polymer Solutions

T. P. LODGE

Department of Chemistry, University of Minnesota, 207 Pleasant St. SE., Minneapolis, MN 55455-0431

(Received August 18, 1995; in final form December 27, 1995)

Applications of dynamic light scattering to the characterization of multicomponent polymer solutions are described. Examples include block copolymers in a selective solvent, which can aggregate into micellar structures; block copolymers in a neutral solvent, in which an unanticipated mode due to chain diffusion appears; probe diffusion in refractive index-matched matrix solutions. The underlying linear response theory is summarized, and the main experimental aspects are noted.

KEY WORDS Dynamic light scattering, multicomponent polymer solutions, micelles, block copolymers, polymer diffusion

INTRODUCTION

Light scattering has been a useful polymer characterization tool for fifty years. Measurements of the scattered intensity I_s from dilute solutions can provide information on the solvent quality, through the osmotic second virial coefficient, on the chain radius of gyration R_g though the dependence on scattering angle, and the weight-average molecular weight M_w in the dual limits of zero concentration and zero angle. If the refractive index increment $\partial n/\partial c$ is known, then the measurement of M_w is absolute, independent of molecular weight distribution or polymer architecture. This fact has contributed to the growing application of light scattering detectors in size exclusion chromatography [1]. Dynamic light scattering (DLS) is a closely related technique that has been employed for thirty years [2,3]. In this experiment the temporal fluctuations $\delta I_s(t)$ about the mean I_s are examined. These fluctuations reflect changes in the spatial distribution of scattering molecules, and thus provide information on molecular motions.

The addition of a time axis to the light scattering experiment opens up a wide range of new possibilities. For example, mixtures of molecules of comparable scattering power but different mobilities can be resolved; molecular weight distribution information can thus be obtained. Also, the state of aggregation of surfactants or copolymers can be assessed. Commercial correlators utilized in DLS instruments typically provide a time window from

---

Presented at the 8th International Symposium on Polymer Analysis and Characterization, Sanibel Island, Florida, May 1995.

10^{-6} to 10^2 s or more, which nicely covers the range associated with isolated polymer motions in small molecule solvents (10^{-6} – 10^{-3} s) up to more concentrated solutions, melts, or aggregates. The role of DLS in polymer analysis falls in the domain of physical, as opposed to chemical characterization. Although precise information about dynamic processes can be obtained, interpretation of the data in terms of molecular structure and interactions requires a reliable model. Fortunately, many such models are available.

This paper concerns the application of DLS to multicomponent systems, which is an area of great current interest. "Multicomponent" in this context means three or more chemical species in the sample; examples include polymer blend solutions, block copolymer solutions, binary mixtures with added surfactant, and globular particles or proteins in polymer solutions. The next section provides a brief summary of the underlying theory, and then some of the experimental aspects are described. The results and discussion section explores several examples of the use of DLS, focusing in particular on (i) tracer diffusion in polymer mixtures, and (ii) block copolymers in nonselective solvents.

BACKGROUND

The fundamental quantity of interest in DLS is the dynamic structure factor $S(q,t)$ defined by

$$S(q,t) \equiv \frac{1}{N^2}\sum_j^N \sum_k^N \left\langle b_j b_k \exp[-i\mathbf{q} \bullet (\mathbf{r}_j(t) - \mathbf{r}_k(0))]\right\rangle \qquad (1)$$

where r_j is the position of scattering center j, b_j is the associated scattering strength, and q is the magnitude of the scattering vector, given by $(4\pi n/\lambda)\sin(\theta/2)$, where θ is the scattering angle and λ is the wavelength of light. The exponential term accounts for the phase difference between light scattered from two centers, and N is the number of scatterers. Consequently, this sum represents the superposition at the detector of the waves scattered by all the molecules in the scattering volume. The average $\langle \ldots \rangle$ is taken over the appropriate probability distribution of $\mathbf{r}_j(t)$.

Information about dynamics is obtained from time-autocorrelation functions of the scattered field. In particular, the normalized electric field correlation function is

$$\begin{aligned} g^{(1)}(q,t) &= \frac{<E_s(t)E_s{}^*(t+\tau)>}{<I_s(\tau)>} \equiv \frac{1}{<I_s>} \lim_{T\to\infty} \frac{1}{T}\int_0^T E_s(\tau)E_s{}^*(t+\tau)d\tau \\ &= \frac{S(q,t)}{S(q,0)} \end{aligned} \qquad (2)$$

where $E_s(t)$ represents the instantaneous scattered field on the detector. However, the measured quantity is the (normalized) intensity correlation function

$$g^{(2)}(q,t) = \frac{<I_s(\tau)I_s(t+\tau)>}{<I_s{}^2>} = 1 + \beta |g^{(1)}(q,t)|^2 \qquad (3)$$

where β is an instrument constant between 0 and 1, called the coherence factor. The second equality in Equation (3) is the Siegert relation, which requires that the scattered electric field be a Gaussian random variable [2,3]. This condition is fulfilled in most DLS applications from fluids, but may fail for nonergodic systems such as gels and glasses [4]. Equation (3) indicates that there is a direct relation between $g^{(2)}(q,t)$ and $S(q,t)$.

For a one-component fluid, all the b_j values are identical, and there will be no scattering, except for density fluctuations. In a two-component, incompressible fluid, there is one concentration variable. For polymer solutions, this variable can be taken as the polymer concentration, c; the dynamic scattering reflects the rise and decay of spontaneous concentration fluctuations with wavevector $\boldsymbol{q}$. The dynamics reflect mutual diffusion, and $S(q,t) = S(q,0)\exp[-\Gamma t]$, where the decay rate $\Gamma = q^2 D_m$, with D_m the mutual diffusion coefficient. The linear dependence on q^2 reflects the fact that the decay time for a fluctuation ($1/\Gamma$) increases as the square of the associated lengthscale ($1/q$), following Fick's law. In the limit of non-interacting particles, that is, as $c \to 0$, D_m approaches the translational diffusion coefficient D_o, which can be directly related to the hydrodynamic radius R_h through the Stokes-Einstein relation:

$$D_0 = \frac{kT}{6\pi\eta R_h} \tag{4}$$

For a sample comprising a distribution of molecular weights, or radii, the field correlation function can be written

$$g^1(q,t) = \int_0^\infty G(\Gamma)\exp(-\Gamma t)\,d\Gamma \tag{5}$$

where $G(\Gamma)d\Gamma$ is the distribution of decay rates, appropriately weighted by scattering power. Equation (5) underlies the application of DLS to particle sizing, as the relation between $G(\Gamma)$ and the size distribution can be calculated for particles of known composition and shape.

For a three-component system, two independent composition variables are necessary, and consequently one expects $S(q,t)$ to be represented by the sum of two exponentials. The two decay rates will be eigenvalues of a 2 × 2 matrix, where the eigenvectors correspond to the two orthogonal composition variables. In general, one may not know exactly what these "normal modes" are, but in many cases they can be reasonably approximated, as will be discussed in more detail later.

EXPERIMENTAL

Samples and Solutions

The synthesis and characterization of the polymer samples have been previously described [5–8]. Solvents (spectrograde quality or higher) were generally used as received. Dilute solutions were prepared gravimetrically, by direct addition of polymer and solvent. More concentrated solutions were prepared by controlled evaporation of solvent, for example under flowing, filtered dry nitrogen. All solutions containing poly(vinyl methyl ether) (PVME) or polyisoprene (PI) also contained antioxidant, at about 0.5% by weight of polymer. Solvents were filtered prior to use, and solutions were filtered through 0.22- or 0.45-

μm filters into scrupulously de-dusted scattering cells. The cells were fashioned from 12-mm o.d. pyrex tubing, and hand-selected for optical clarity.

Apparatus

Correlation functions were obtained on either of two instruments, as previously described [9,10]; each employs an Ar^+ laser operating at 488 nm. Scattering angles ranged from 30 to 135 degrees. Temperatures were controlled to ±0.1°C using a flow-through controller. Two correlators were employed: a Brookhaven 2030AT, with 256 channels and up to four delay times, and a Brookhaven 9000AT, with 522 channels spaced from 100 ns to 1300 s.

Analysis

Correlation functions were analyzed in various ways. In all cases, the inverse Laplace transform routine CONTIN was applied, to obtain an estimate of $G(\Gamma)$ [11]. This program is particularly valuable when there are two or more decay modes in $g^{(2)}(q,t)$ (*i.e.*, peaks in $G(\Gamma)$). However, Laplace inversion is an ill-posed problem, admitting many possible solutions for a given data set, particularly in the presence of noise. Thus, when there is only one mode, the method of cumulants is generally preferred [12]. If there is reason to expect another functional form to represent the data, such as a sum of two exponentials or a stretched exponential, then these can be fit to the data by nonlinear regression. In all cases, it is important to establish consistency among fits to data obtained at different scattering angles for a given sample, and for a given sample at different temperatures or concentrations.

Example

A polystyrene-polyisoprene (PS-PI) diblock copolymer with $M_w = 3.4 \times 10^5$, $M_w/M_n = 1.08$, and containing 50 wt% PS, was dissolved in cyclohexane at a weight fraction of 0.005. Cyclohexane is a good solvent for PI, but a theta solvent for PS at 35°C. Figure 1a shows correlation functions obtained at a scattering angle of 90°, at both 10 and 30°C. The higher temperature curve is close to a single exponential decay, whereas the lower temperature curve is shifted to longer times, and is broader. Figure 1b displays the corresponding Laplace inversions, in the "equal area" representation ($\Gamma G(\Gamma)$ vs. log Γ). At the higher temperature, a single peak is evident, whereas at the lower temperature, two modes emerge. In all cases, the mean decay rates associated with each mode are linear in q^2, indicating that they reflect diffusive processes. Figure 2 shows the decay rates of the two modes at 10 °C, and the associated diffusivities. Through Equation (4), values of the corresponding hydrodynamic radii of 18 and 240 nm are assigned to the fast and slow processes, respectively. The former agrees very well with the value of 16 nm obtained for the isolated chain in the neutral good solvent toluene [6], and with the value of 15 nm obtained in cyclohexane at 30°C. The latter is substantially greater, and is attributed to the formation of micelles as the PS becomes insoluble in the solvent. These micelles are expected to be roughly spherical in shape, given the magnitude of R_h and the narrowness of the associated peak in Figure 1b, but this can not be proven on the basis of these data alone.

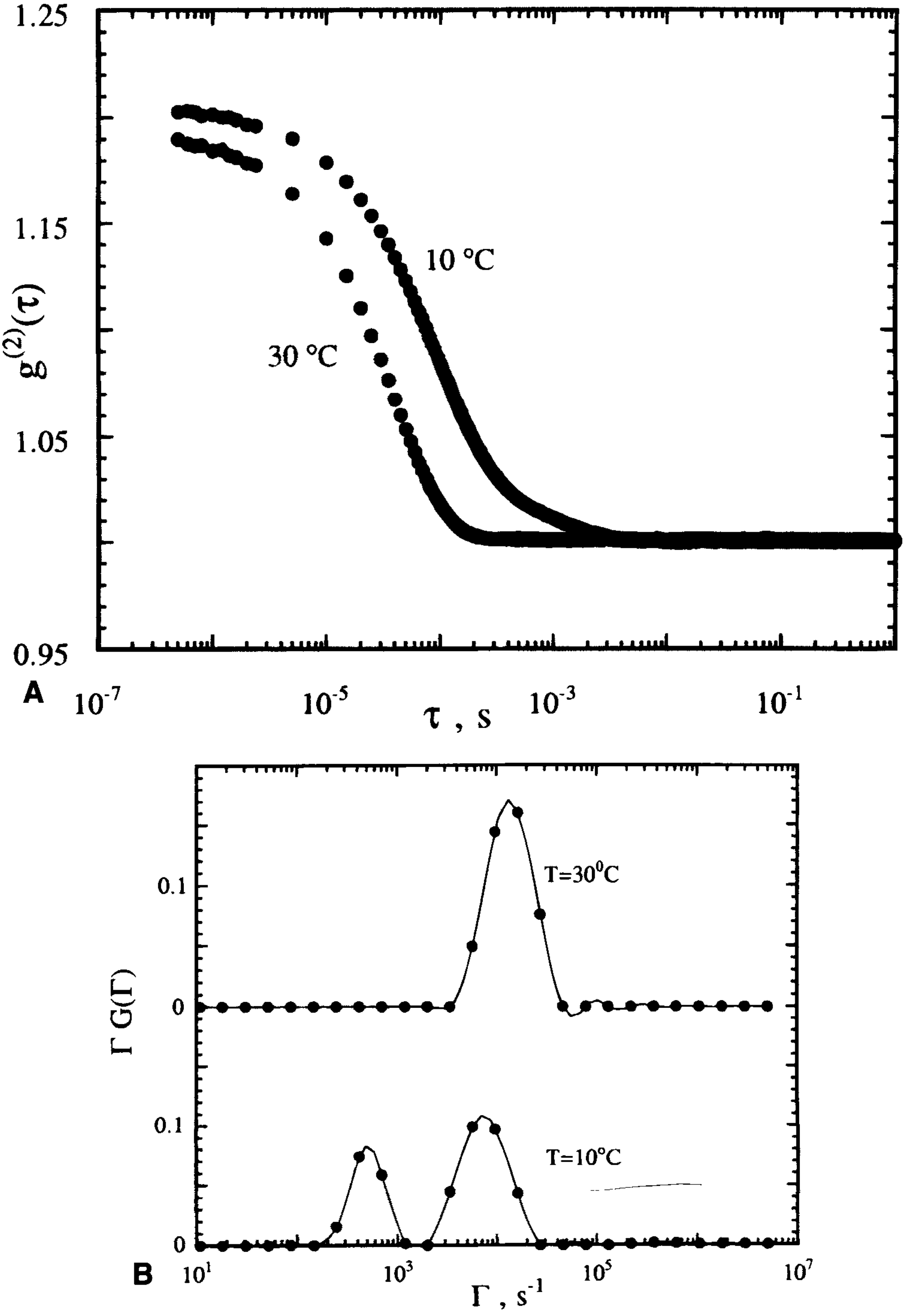

FIGURE 1 (a) Intensity correlation functions for a symmetric PS-PI diblock copolymer in cyclohexane, c = 0.005 g/g, for a scattering angle of 90°, at 10 and 30°C, and (b) the corresponding Laplace inversions, indicating the appearance of micelles at the lower temperature.

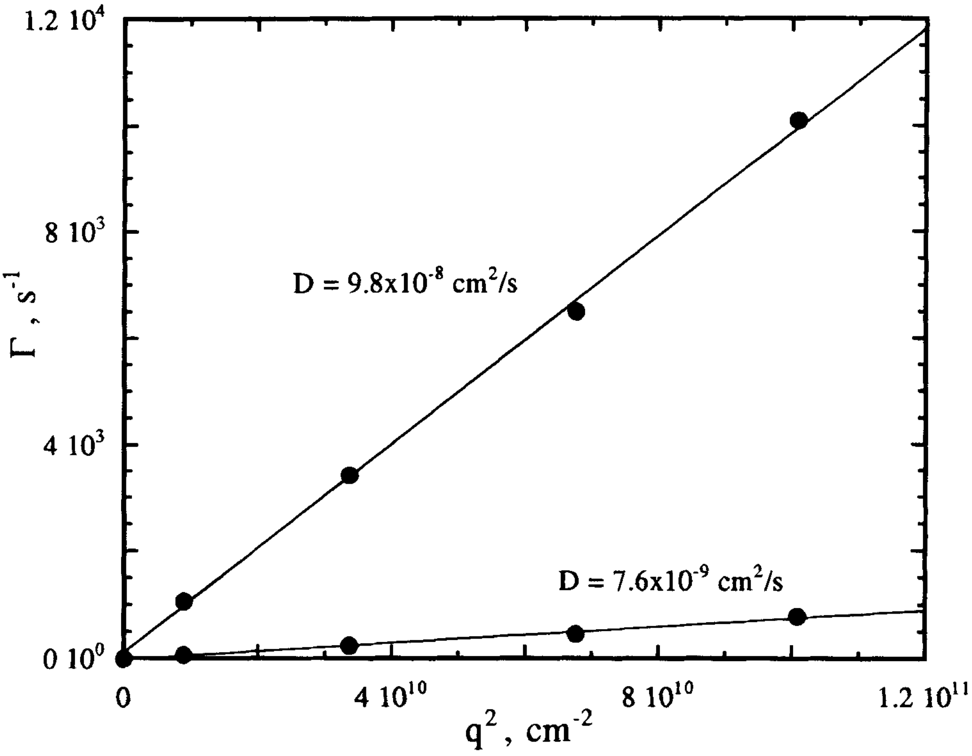

FIGURE 2 Dependence of decay rate on squared wavevector for the solution in Figure 1, at 10°C.

RESULTS AND DISCUSSION

Polymer Blend Solutions

Consider a ternary system containing polymer A, polymer B, and solvent, and let c_A and c_B denote the polymer concentrations; incompressibility requires $c_A + c_B = 1 - c_S$. If both c_A and c_B are $<< 1$, one might expect δc_A and δc_B to be uncoupled, and consequently the two decay modes would reflect the diffusivities of the two species. This is, indeed, the case, but it is important to recognize that the decay rates must be well separated (*e.g.*, by a factor of at least three) in order to be resolved. However, ternary solutions dilute in both polymer components are relatively uninteresting. At higher concentrations, in the so-called semidilute regime, δc_A and δc_B are less likely to be independent. "Semidilute" refers to a solution in which c_A and/or $c_B < 0.2$, but is sufficiently large that coil overlap is achieved; the coil overlap concentration c* is typically of order 0.01. Here, a particularly appealing possibility is that the independent concentration variables are the total polymer concentration, $c_A + c_B$, and the differential polymer concentration, $c_A - c_B$. Fluctuations in the former relax by cooperative diffusion, that is, mutual diffusion of polymer and solvent, and the latter by interdiffusion, that is, mutual diffusion of polymer A and B. This picture provides a reasonable, albeit approximate, description of the DLS results for two polymers in a common good solvent [13–15]. The cooperative mode depends on the polymer/solvent interaction, and increases in rate with increasing c. The interdiffusion mode, however, reflects the thermodynamics of A–B interactions, which are usually effectively repulsive. Indeed, as c_A and c_B increase, a phase boundary is usually encountered, resulting in liquid-liquid phase separation. The rate of interdiffusion decreases markedly as this boundary is approached.

The relative amplitudes of the two modes are also important. Both depend on the corresponding refractive index increments, or optical contrast. For the cooperative mode, one expects

$$A_c \propto \left(c_A \left(\frac{\partial n}{\partial c} \right)_A + c_B \left(\frac{\partial n}{\partial c} \right)_B \right)^2 \tag{6}$$

If a solvent is chosen with refractive index intermediate between that of the two polymers, $(\partial n/\partial c)_A$ and $(\partial n/\partial c)_B$ will usually be of opposite sign. By appropriate selection of conditions, a zero-average contrast (ZAC) solvent can be found, in which the cooperative mode amplitude vanishes. Another important possibility is to chose a solvent such that $(\partial n/\partial c)B = 0$; under such "index-matching" conditions, only fluctuations in c_A are visible. Note, however, that the refractive index depends on λ and T, and thus these two parameters must also be specified to achieve exact index-matching conditions.

A particularly useful situation arises when A, the "tracer" or "probe", is present in very small amounts but has large $(\partial n/\partial c)$, and B, the "matrix" is quite concentrated but is index-matched to the solvent. In such a case $S(q,t)$ reduces to a single mode, characteristic of the diffusion of the tracer through the matrix. This technique has been used extensively to investigate the mechanisms of diffusion in non-dilute solutions. For example, we have used polystyrene as the tracer, and poly(vinyl methyl ether) in either toluene or o-fluorotoluene as the matrix [5,7–9,16,17]. This system has an additional advantage, in that PS and PVME are miscible in all proportions, and thus phase separation does not occur at the measurement T. Accordingly, matrix concentrations as high as 0.30 were achieved, such that the diffusivity of the PS chains had decreased by as much as 10^5 from the infinite dilution result. Experimental correlation functions were unimodal in all cases, as expected, and the resulting mean decay rates were linearly proportional to q^2. Both linear and star-branched PS chains were utilized, to test the applicability of the reptation hypothesis to nondilute solutions. The reptation model conjectures that an individual chain relaxes stress by diffusing predominantly along its own contour, through the constraints provided by the entangling matrix chains [18,19]. If this is correct, a branched polymer should diffuse considerably less rapidly than a linear chain of comparable R_h [20]. Subsequently, cross-linked PVME matrices (*i.e.*, gels) were employed, as a further test of the model [16,17]. A probe chain that reptates should exhibit a diffusivity independent of the mobility of the matrix chains; cross-linking the matrix should have no effect. In general, the data support the basic concept, but also demonstrate that a clear reptation regime does not exist in semidilute solutions.

In a further study, PS latex spheres ($R_h \approx 200$ nm) were dispersed in the same matrix, to investigate reported failures of the Stokes-Einstein relation (Equation (4)) in semidilute solutions [5]. The issue is whether in this concentration regime the probe particle senses the macroscopic viscosity of the suspending fluid. Indeed, we observed that Equation (4) did break down near c^* for the matrix, but that it was apparently followed again at higher concentrations. The origin of the interesting departure from Equation (4) near c^* is not fully understood. However, qualitatively it can be interpreted in the following way. At any instant in time for $c > c^*$, the matrix appears as a network, with a mesh size that decreases with increasing concentration. The matrix viscosity depends on the ability of the chains to move past one another. A molecule smaller than the mesh will move through relatively easily, whereas one much larger cannot. Thus, larger spherical probes should be more apt to follow Equation (4). However, near c^* the solution does not resemble a network, but at any instant is spatially inhomogeneous on the length scale of the chain size. Consequently, particles can move more rapidly than expected. In the reptation model, a linear chain should move increasingly faster than Equation (4) predicts as concentration increases, because it is able to snake through the mesh. Figure 3 shows the results for solvent, linear PS of two different lengths, a 3-arm star PS, and the spheres, represented as smooth curves plotted in reduced format. The ordinate is the product of D and η, normalized to the infinite dilution limit, so

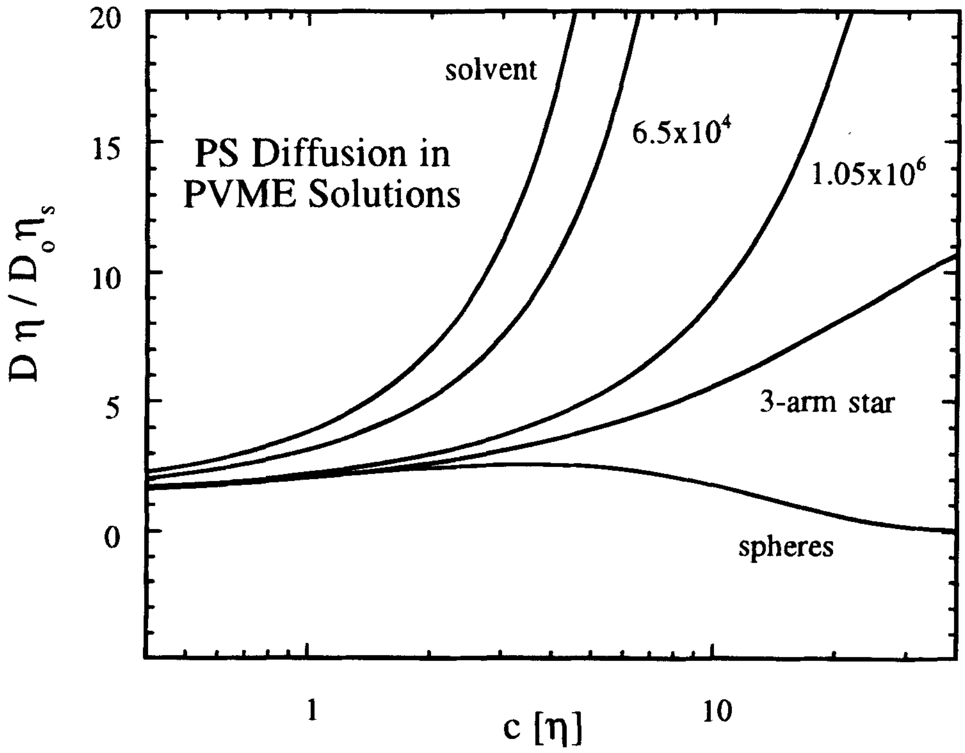

FIGURE 3 Normalized product of diffusivity and viscosity for various probes in poly(vinyl methyl ether) solutions, with a matrix molecular weight of 1.3×10^6. The actual data are represented by smooth curves (products of stretched exponentials) for clarity. The probes are the solvent, linear PS with the indicated molecular weights, a three-arm PS star with $M = 1.19 \times 10^6$, and a PS latex sphere with $R \approx 200$ nm.

adherence to Equation (4) would correspond to a constant value of one. The abscissa is the product of matrix concentration and intrinsic viscosity, which is effectively c/c*. The data are in at least qualitative accord with the reptation model when c/c* >> 1; the linear chains move more rapidly than the star, whereas the spheres return toward Stokes-Einstein behavior. (The tendency of the sphere curve to approach 0 at large *c* is an artifact of the interpolation formulæ employed to represent the data).

Block Copolymer Solutions

Consider an A–B diblock copolymer in a nonselective solvent. Unlike the case of PS-PI in cyclohexane illustrated previously, micellization should not occur, but at sufficiently high *c* or *M* the system will undergo an order-disorder transition (ODT) to a periodic microphase-separated structure. We will only consider solutions in the disordered state. Although thermodynamically there are two components, from a scattering perspective there are three, and consequently $S(q,t)$ should comprise two modes [5,21,22]. The cooperative mode will carry over directly from the blend solution case, corresponding to the relaxation of polymer/solvent concentration fluctuations. However, interdiffusion is replaced by an "internal relaxation" mode, whereby there are local fluctuations in refractive index due to relative motion of the two blocks. Such a mode is characterized by a decay rate independent of q, and typically has very small amplitude.

Extensive measurements on such systems are generally not in agreement with this picture; a third mode, typically larger in amplitude than either of the other two, consistently appears [6,23–27]. This mode is diffusive ($\Gamma \sim q^2$), and the diffusivity is close to the translational diffusion of the chains. How does this mode arise? It is thought to reflect heterogeneity in composition, that is, chain-to-chain fluctuations in scattering power due to different relative numbers of A and B monomers [28]. If the block copolymers were absolutely identical, it would be impossible to generate an A–B composition fluctuation for any wavelength much greater than the chain size. However, due to the inevitable distribution of chain length and composition, even in an ideal living anionic polymerization, such fluctuations are possible. They will relax by exchange of A-rich and B-rich chains, that is, by translational diffusion.

As an example, Figure 4 shows a Laplace inversion obtained for the same PS-PI diblock considered in Figures 1 and 2, but in the neutral good solvent toluene [6]. The concentration is such that the solution lies in the semidilute regime. Three modes are clearly resolved. The fastest and slowest are both diffusive, whereas the intermediate mode appears to have decay rate independent of q. Figure 5 shows the concentration dependence of the two diffusive modes. The faster process, assigned to cooperative diffusion, increases in rate with increasing concentration, as expected for mutual diffusion, and indeed the data are in quantitative agreement with measurements of PS homopolymers in toluene. In other words, the copolymer nature of the chains is irrelevant to this process. The slower process, assigned to the heterogeneity mode, decreases in rate rapidly with concentration, and is in close agreement with translational diffusion as measured by pulsed-field gradient NMR. This result provides strong support for the explanation based on compositional heterogeneity.

The intermediate mode, assigned to the internal relaxation described above, is hard to resolve consistently in the presence of the other two, stronger modes (the example

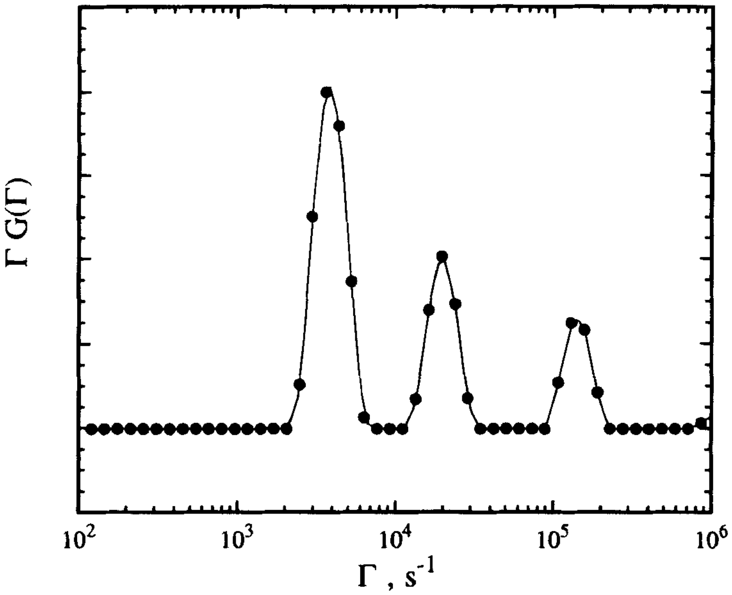

FIGURE 4 Laplace inversion of an intensity correlation function for the same PS-PI diblock as in Figures 1 and 2, only dissolved in the neutral good solvent toluene, with c = 0.0489 g/g. The three modes in order of increasing rate correspond to chain diffusion (heterogeneity mode), viscoelastic relaxation (internal mode), and cooperative diffusion.

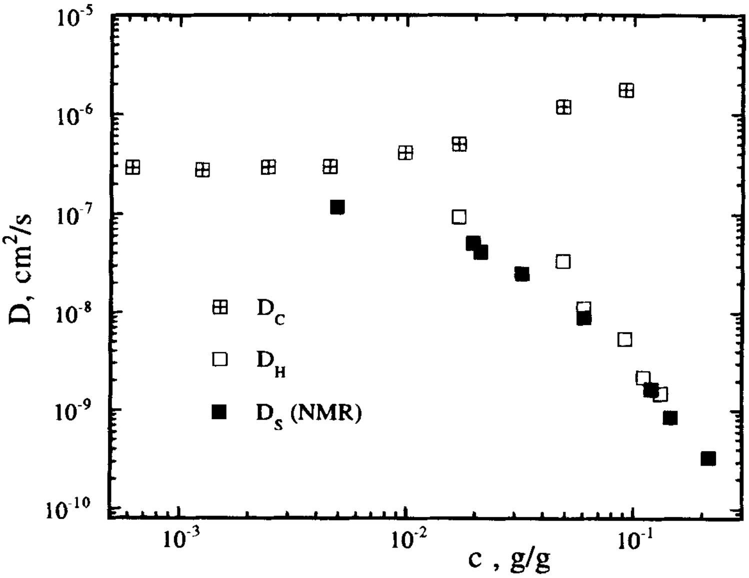

FIGURE 5 Concentration dependence of the cooperative and heterogeneity mode diffusion coefficients for the PS-PI diblock in toluene. Also shown are the self-diffusion coefficients measured by pulsed-field gradient NMR.

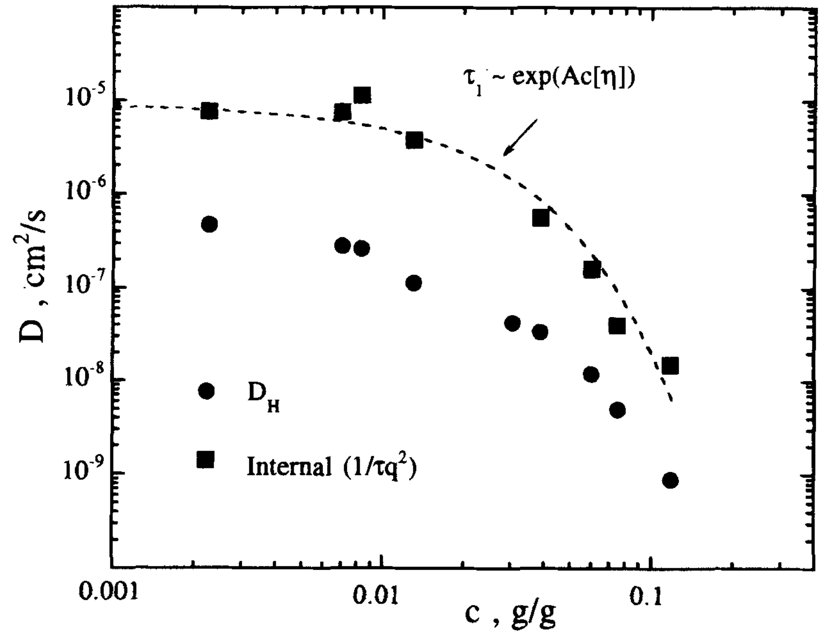

FIGURE 6 Concentration dependence of the internal mode relaxation time and the heterogeneity mode diffusion coefficient for the PS-PI diblock in a zero-average contrast solvent, prepared by blending toluene and α-chloronaphthalene.

in Figure 4 is uncharacteristic in this respect). Consequently, analogous measurements were made in a zero-average contrast solvent composed of toluene and α-chloronaphthalene [29]. In this case the cooperative mode vanishes, and the internal mode, though still weak, could be resolved. Its concentration dependence is shown in Figure 6. Also shown is the estimated concentration dependence of the longest viscoelastic relaxation time for this polymer; the agreement also provides strong support for the mode assignments.

ACKNOWLEDGMENTS

This work was supported by the National Science Foundation through Grant DMR-9019907, and by the Center for Interfacial Engineering, an NSF-supported Engineering Research Center at the University of Minnesota. The willingness of B. Lam and Z. Liu to provide the data in Figures 1 and 2 is appreciated.

REFERENCES

1. P. J. Wyatt, *Anal. Chim. Acta*, **272**, 1 (1993).
2. B. J. Berne and R. Pecora, *Dynamic Light Scattering*; Wiley: New York, 1976.
3. B. Chu, *Laser Light Scattering*; Academic Press: San Diego, 1991; 2nd ed.
4. P. N. Pusey and W. van Megen, *Physica A*, **157**, 705 (1990).
5. J. Won, C. Onyenemezu, W. G. Miller, and T. P. Lodge, *Macromolecules*, **27**, 7389 (1994).
6. C. Pan, W. Maurer, Z. Liu, T. P. Lodge, P. Stepanek, E. D. von Meerwall, and H. Watanabe, *Macromolecules*, **28**, 1643 (1995).
7. T. P. Lodge, P. Markland, and L. M. Wheeler, *Macromolecules*, **22**, 3409 (1989).
8. L. M. Wheeler and T. P. Lodge, *Macromolecules*, **22**, 3399 (1989).
9. T. P. Lodge and P. Markland, *Polymer*, **28**, 1377 (1987).
10. M. S. Kent, M. Tirrell, and T. P. Lodge, *J. Polym. Sci., Polym. Phys. Ed.*, **32**, 1927 (1994).
11. S. W. Provencher, *Comput. Phys. Commun.*, **27**, 229 (1982).
12. D. E. Koppel, *J. Chem. Phys.*, **57**, 4814 (1972).
13. R. Borsali, M. Duval, and M. Benmouna, *Macromolecules*, **22**, 816 (1989).
14. M. Benmouna, H. Benoit, M. Duval, and A. Z. Akcasu, *Macromolecules*, **20**, 1107 (1987).
15. A. Z. Akcasu, B. Hammouda, T. P. Lodge, and C. C. Han, *Macromolecules*, **17**, 759 (1984).
16. N. A. Rotstein and T. P. Lodge, *Macromolecules*, **25**, 1316 (1992).
17. J. Won and T. P. Lodge, *J. Polym. Sci., Polym. Phys. Ed.*, **31**, 1897 (1993).
18. P. G. de Gennes, *J. Chem. Phys.*, **55**, 572 (1971).
19. P. G. de Gennes, *Scaling Concepts in Polymer Physics*; Cornell Univ. Press: Ithaca, 1979.
20. P. G. de Gennes, *J. Phys. (Paris)*, **36**, 1199 (1975).
21. M. Benmouna, H. Benoit, R. Borsali, and M. Duval, *Macromolecules*, **20**, 2620 (1987).
22. M. Benmouna, M. Duval, and R. Borsali, *J. Polym. Sci., Polym. Phys. Ed.*, **25**, 1839 (1987).
23. N. P. Balsara, P. Stepanek, T. P. Lodge, and M. Tirrell, *Macromolecules*, **24**, 6227 (1991).
24. H. Haida, J. P. Lingelser, Y. Gallot, and M. Duval, *Makromol. Chem.*, **192**, 2701 (1992).
25. R. Borsali, E. W. Fischer, and M. Benmouna, *Phys. Rev. A.*, **43**, 5732 (1991).
26. C. Konak and J. Podesva, *Macromolecules*, **24**, 6502 (1991).
27. T. Jian, S. H. Anastasiadis, A. N. Semenov, G. Fytas, K. Adachi, and T. Kotaka, *Macromolecules*, **27**, 4762 (1994).
28. A. N. Semenov, G. Fytas, and S. H. Anastasiadis, *Polym. Prepr. (Am. Chem. Soc., Div. Polym. Chem.)*, **35** (1), 618 (1994).
29. Z. Liu, C. Pan, P. Stepanek, T. P. Lodge, *Macromolecules*, **28**, 3221 (1995).